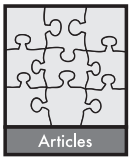

Journal of Avian Biology 48: 932–940, 2017
doi: 10.1111/jav.01163

Subject Editor: Martin Paeckert. Editor-in-Chief: Thomas Alerstam. Accepted 31 December 2016

Phylogeny of penduline tits inferred from mitochondrial and microsatellite genotyping

Hossein Barani-Beiranvand, Mansour Aliabadian, Martin Irestedt, Yanhua Qu, Jamshid Darvish, Tamás Székely, René E. van Dijk and Per G. P. Ericson

H. Barani-Beiranvand, M. Aliabadian (aliabadi@um.ac.ir) and J. Darvish, Dept of Biology, Faculty of Science, Ferdowsi Univ. of Mashhad, Iran Mashhad, Khorasan-e Razavi, Mashhad, Iran. MA also at: Research Dept of Zoological Innovation (RDZI), Inst. of Applied Zoology, Ferdowsi Univ. of Mashhad, Mashhad, Iran. JD also at: Research Dept of Rodentology, Inst. of Applied Zoology, Ferdowsi Univ. of Mashhad, Mashhad, Iran. – M. Irestedt, Dept of Bioinformatics and Genetics, Swedish Museum of Natural History, Stockholm, Sweden. – Y. Qu, Inst. of Zoology, Chinese Academy of Sciences, Beijing, China. – T. Székely, Dept of Biology and Biochemistry, Univ. of Bath, Bath, UK. – R. E. van Dijk, Dept of Animal and Plant Sciences, Univ. of Sheffield, Sheffield, UK. – P. G. P. Ericson, Dept of Zoology, Swedish Museum of Natural History, Stockholm, Sweden.

Penduline tits (*Remiz* spp.) are renowned for their diverse mating and parenting strategies, and are a well-studied system by behavioural ecologists. However, the phylogenetic relationships and species delimitations within this genus are poorly understood. Here, we investigate phylogenetic relationships within the genus *Remiz* by examining the genetic variation in the mitochondrial cytochrome-*b* gene of 64 individuals and in ten autosomal microsatellite markers from 44 individuals. The taxon sampling includes individuals from all currently recognized species (*R. pendulinus*, *R. macronyx*, *R. coronatus*, and *R. consobrinus*) and most subspecies in the Palearctic region. We showed that *R. coronatus* and *R. consobrinus* are genetically well differentiated and constitute independent evolutionary lineages, separated from each other and from *R. pendulinus*/*macronyx*. However, we found no evidence for significant differentiation among *R. pendulinus*/*macronyx* individuals in mtDNA haplotypes and only marginal differences between *R. pendulinus* and *R. macronyx* in microsatellite markers. Hence, based on present data our recommendation is to treat *R. pendulinus* and *R. macronyx* as conspecific and *R. coronatus* and *R. consobrinus* as separate species.

Species are central units in biology, but what constitutes a species is sometimes contested. Traditionally, species descriptions are built on phenotypic traits of which the genetic basis is often poorly known (Price 2008). In birds there are many variable species complexes whose taxonomy remains disputed, mainly because it has been difficult to assess whether the morphological variation represents an early stage of diversification into separate species or if it simply represents standing morphological variation within a single panmictic meta-population. To better understand speciation processes and phenotypic diversity, several of these presumably young and contested avian species complexes have recently been subject to extensive molecular studies (Ottvall et al. 2002, Rheindt et al. 2011, Mason and Taylor 2015). Genetic data have, for example, been used to study the Holarctic redpoll complex *Carduelis flammea* that traditionally has been divided into two or three species based on phenotypic variation in plumages. However, the genetic data suggest that this complex constitutes a single species and that the phenotypic variation is merely a result of differences in gene expression (Mason and Taylor 2015). Another example is the carrion *Corvus corone corone* and hooded crows *C. c. cornix* where genomic data have shown that there is extensive gene flow between these two subspecies, while assortative mating maintains the stable plumage differences between these two subspecies (Poelstra et al. 2014).

The penduline tit genus *Remiz* is distributed across the Palearctic region and occurs in diverse habitats, from reed marshes to arid semi-deserts. They are common in south-eastern and central Europe, as well as central and east Asia (Isenmann 1987, Newton 2010) (Fig. 1). Several studies have investigated the morphological (Snow 1967, Eck and Martens 2006) and behavioural (Persson and Öhrström 1989, van Dijk et al. 2010a, b) variation within this genus. The Eurasian penduline tit *Remiz pendulinus* is a small (body mass 9–10 g), sexually dimorphic passerine bird. Males are more brightly coloured than females with a dark red-brown mantle, reddish spots on the breast, and a brighter grey-white crown and a wider mask than females (Cramp and Perrins 1993). This species exhibits a highly variable mating and parental care system, and it has been argued that sexual conflict over parental care is the main driver of such phenotypic variation (Szentirmai et al. 2007, van Dijk et al. 2010b, 2012).

Previous research has combined all *Remiz* taxa as one wide-ranging polytypic species, *Remiz pendulinus* with seven to 12 subspecies (Portenko 1955, Snow 1967, Dickinson 2003), while others recognize four species, i.e. the Eurasian

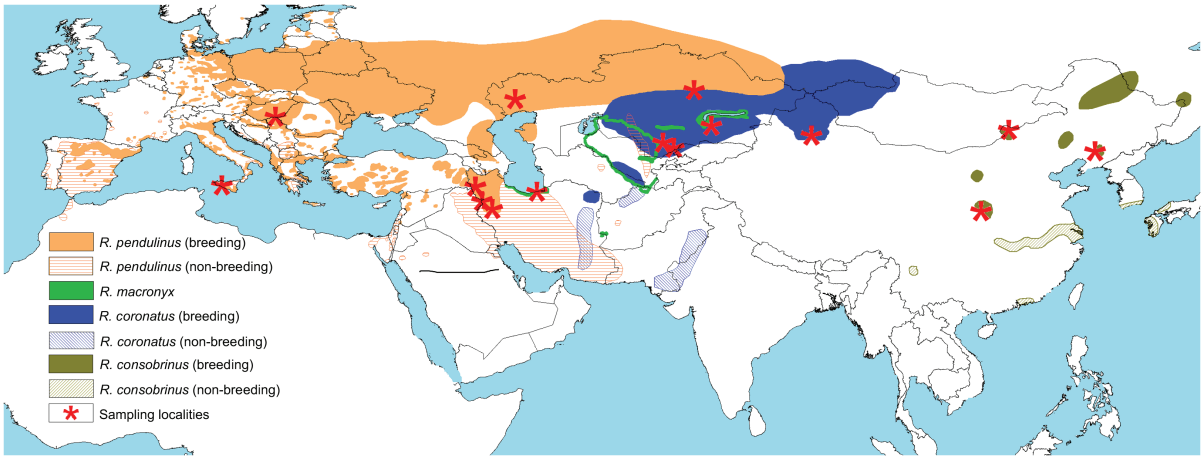

Figure 1. Distribution map of the genus *Remiz* and recognized taxa; *R. pendulinus* (light brown: breeding, horizontal lines: non-breeding), *R. macronyx* (green), *R. coronatus* (blue: breeding, upward diagonal lines: non-breeding), and *R. consobrinus* (olive: breeding, downward diagonal lines: non-breeding). Sampling localities (red stars) are given. Distribution map source: BirdLife international (2015) with small modifications.

penduline tit *R. pendulinus* (*R. p. pendulinus*, *R. p. menzbieri*, *R. p. jaxarticus*, and *R. p. caspius*), the black-headed penduline tit *R. macronyx* (*R. m. macronyx*, *R. m. neglectus*, *R. m. nigricans*, and *R. m. ssaposhnikowi*), the white-crowned penduline tit *R. coronatus* (*R. c. coronatus* and *R. c. stoliczkae*), and the Chinese penduline tit *R. consobrinus* (monotypic) (Harrap and Quinn 1996, Madge 2008). Based on DNA-DNA hybridization, Sibley and Monroe (1990) recognized three species by lumping *R. pendulinus* with *R. macronyx*, an approach adopted by Eck and Martens (2006). Cramp and Perrins (1993) and Dickinson and Christidis (2014) recognized three species but instead lumped *R. coronatus* with *R. consobrinus* into one species.

In this study, we investigate the phylogenetic structure within the genus *Remiz* by sequencing the mitochondrial cytochrome-*b* gene and genotyping ten microsatellite loci from a geographically broad taxon sampling encompassing all previously described species. *Remiz pendulinus* and *R. macronyx* exhibit distinctive differences in plumage and morphology, yet have often been suggested to be conspecific and are known to hybridize along the Caspian Sea (Harrap and Quinn 1996, Madge 2008). We have thus sampled these taxa particularly densely and included samples from the area where they are known to hybridize.

Methods

Taxon sampling, DNA extraction and sequencing

Blood (ca 10 µl) or feather samples were collected from 61 adult birds originating from across the Palearctic region (Fig. 1), including 32 individuals of *R. pendulinus* (*R. p. pendulinus* (n = 4), *R. p. menzbieri* (n = 27), and *R. p. caspius* (n = 1)), 21 individuals of *R. macronyx* (*R. m. macronyx* (n = 2), *R. m. neglectus* (n = 18), and *R. m. ssaposhnikowi* (n = 1)), 6 individuals of *R. coronatus* (*R. c. coronatus* (n = 4) and *R. c. stoliczkae* (n = 2)), and 5 individuals of *R. consobrinus*. Genomic DNA was extracted using the QIAamp™ DNA Mini Extraction Kit (Qiagen) following the manufacturers' protocol. We amplified a 843 base-pair (bp) fragment of the mitochondrial cytochrome-*b* gene using the primer pair: CytbRemizF1b (ACCCCATAATAAGGAGAAGGRTT) and CytbRemizR4 (AAGAGCAAGTTTACTAAATGTAAGC). The specific primers were designed at the Swedish Museum of Natural History for this study. In the final data set we also included sequences downloaded from GenBank from additional *Remiz* samples (i.e. *Remiz consobrinus*: GenBank Accession numbers: HM185374, HM185375, KC463856), and sequences obtained from species in closely-related genera (i.e. Cape penduline tit *Anthoscopus minutus*: AF347970; verdin *Auriparus flaviceps*: AF347969 and great tit *Parus major*: AY495412). The common magpie *Pica pica* (JQ393938) was used to root the tree. All new DNA sequences generated for this study have been deposited in GenBank and the accession numbers are provided in Table 1.

Microsatellite genotyping

Twenty-six *R. pendulinus* and 18 *R. macronyx* samples were genotyped using ten polymorphic microsatellites (Mészáros et al. 2008, Dawson et al. 2010, 2013; Supplementary material Appendix 1). All markers were amplified in three multiplex sets: (A) *Remiz*-01, *Remiz*-07, and *Remiz*-09, (B) *Remiz*-10, *Remiz*-18, and CAM-10, (C) TG04-061, TG13-009, TG05-053, and TG13-017. All PCR reactions were conducted in a final volume of 12.5 µl and containing 6.25 µl 2x Qiagen Multiplex PCR Master Mix (Qiagen), 1.25 µl of primer mix, and 2 and 3 µl DNA extract, depending on whether blood or feather samples were used, respectively. Forward primers were fluorescently labeled with VIC (green), NED (yellow), 6-FAM (blue), or PET (red). The PCR thermal profile used for amplifying all the microsatellites started with an initial denaturation at 95°C for 5 min, which was followed by 35 cycles of 95°C for 30 s, 54°C for 30 s and 72°C for 30 s followed by a final extension step at 72°C for 12 min. The samples were run on an ABI Prism 3130xl Genetic Analyzer and scored in GENEMAPPER 4.2 (Applied Biosystems). Micro-checker ver. 2.2.3 (van Oosterhout et al. 2004) was applied to test for possible

Table 1. List of samples used for molecular analysis; GenBank accession numbers listed for cytochrome-*b* sequences. Other accession numbers generated by this study and deposited in GenBank. *: the exact locality is not known.

Code	Species	Subspecies	Country	Region	E	N	Acc. No.
R_cons1	*R. consobrinus*	*consobrinus*	China	Liaonin	123.4	41.84	HM185374
R_cons2	*R. consobrinus*	*consobrinus*	China	Liaoning	123.4	41.84	HM185375
R_cons3	*R. consobrinus*	*consobrinus*	China	Shaanxi	109	34.27	KC463856
Rcons_108	*R. consobrinus*	*consobrinus*	China	Xianghai	112.5	44.5	KY693979
Rcons_109	*R. consobrinus*	*consobrinus*	China	Xianghai	112.5	44.5	KY693980
Rcoro_cor1	*R. coronatus*	*coronatus*	Kazakhstan	Topar	72.82	49.51	KY693981
Rcoro_cor2	*R. coronatus*	*coronatus*	Kazakhstan	Topar	72.82	49.51	KY693982
Rcoro_KA46263	*R. coronatus*	*coronatus*	Kazakhstan	Jabagly	70.29	42.25	KA46263
Rcoro_KA46264	*R. coronatus*	*coronatus*	Kazakhstan	Jabagly	70.29	42.25	KA46264
Rcor_stol_7901	*R. coronatus*	*stoliczkae*	China	Xinjiang	87.63	43.79	KY693983
Rcor_stol_7990	*R. coronatus*	*stoliczkae*	China	Xinjiang	87.63	43.79	KY693984
Rmac_neg1	*R. macronyx*	*neglectus*	Iran	Mazandaran	52.92	36.73	KY693985
Rmac_neg10	*R. macronyx*	*neglectus*	Iran	Mazandaran	52.92	36.73	KY693986
Rmac_neg11	*R. macronyx*	*neglectus*	Iran	Mazandaran	52.91	36.73	KY693987
Rmac_neg12	*R. macronyx*	*neglectus*	Iran	Mazandaran	52.91	36.73	KY693988
Rmac_neg13	*R. macronyx*	*neglectus*	Iran	Mazandaran	52.92	36.73	KY693989
Rmac_neg14	*R. macronyx*	*neglectus*	Iran	Mazandaran	52.92	36.73	KY693990
Rmac_neg15	*R. macronyx*	*neglectus*	Iran	Mazandaran	52.92	36.73	KY693991
Rmac_neg16	*R. macronyx*	*neglectus*	Iran	Mazandaran	52.7	36.59	KY693992
Rmac_neg17	*R. macronyx*	*neglectus*	Iran	Mazandaran	52.63	36.68	KY693993
Rmac_neg18	*R. macronyx*	*neglectus*	Iran	Mazandaran	52.82	36.63	KY693994
Rmac_neg2	*R. macronyx*	*neglectus*	Iran	Mazandaran	53.03	36.7	KY693995
Rmac_neg3	*R. macronyx*	*neglectus*	Iran	Mazandaran	52.75	36.6	KY693996
Rmac_neg4	*R. macronyx*	*neglectus*	Iran	Mazandaran	52.75	36.6	KY693997
Rmac_neg5	*R. macronyx*	*neglectus*	Iran	Mazandaran	52.75	36.6	KY693998
Rmac_neg6	*R. macronyx*	*neglectus*	Iran	Mazandaran	52.75	36.6	KY693999
Rmac_neg7	*R. macronyx*	*neglectus*	Iran	Mazandaran	52.75	36.6	KY694000
Rmac_neg8	*R. macronyx*	*neglectus*	Iran	Mazandaran	52.75	36.6	KY694001
Rmac_neg9	*R. macronyx*	*neglectus*	Iran	Mazandaran	52.75	36.6	KY694002
Rm_macro_1901	*R. macronyx*	*macronyx*	Kazakhstan	Turkestan	68.93	42.90	KY694003
Rm_macro_1907	*R. macronyx*	*macronyx*	Kazakhstan	Turkestan	68.93	42.90	KY694004
Rm_ssapo_KA46261	*R. macronyx*	*ssaposhnikowi*	Kazakhstan	Topar	75.01	45.03	KY694005
Rpen_menz1	*R. pendulinus*	*menzbieri*	Iran	Kermanshah	47.41	34.55	KY694006
Rpen_menz10	*R. pendulinus*	*menzbieri*	Iran	Hamadan	48.32	34.32	KY694007
Rpen_menz11	*R. pendulinus*	*menzbieri*	Iran	Hamadan	48.32	34.32	KY694008
Rpen_menz12	*R. pendulinus*	*menzbieri*	Iran	Hamadan	48.32	34.32	KY694009
Rpen_menz13	*R. pendulinus*	*menzbieri*	Iran	Hamadan	48.32	34.32	KY694010
Rpen_menz14	*R. pendulinus*	*menzbieri*	Iran	Hamadan	48.32	34.32	KY694011
Rpen_menz15	*R. pendulinus*	*menzbieri*	Iran	Hamadan	48.32	34.32	KY694012
Rpen_menz16	*R. pendulinus*	*menzbieri*	Iran	Hamadan	48.32	34.32	KY694013
Rpen_menz17	*R. pendulinus*	*menzbieri*	Iran	Hamadan	48.32	34.32	KY694014
Rpen_menz18	*R. pendulinus*	*menzbieri*	Iran	Hamadan	48.32	34.32	KY694015
Rpen_menz19	*R. pendulinus*	*menzbieri*	Iran	Hamadan	48.32	34.32	KY694016
Rpen_menz2	*R. pendulinus*	*menzbieri*	Iran	Azerbaijan-e-Sharghi	46.88	39.12	KY694017
Rpen_menz20	*R. pendulinus*	*menzbieri*	Iran	Azerbaijan-e-Sharghi	46.88	39.12	KY694018
Rpen_menz21	*R. pendulinus*	*menzbieri*	Iran	Azerbaijan-e-Gharbi	45.25	37.4	KY694019
Rpen_menz22	*R. pendulinus*	*menzbieri*	Iran	Azerbaijan-e-Gharbi	45.25	37.4	KY694020
Rpen_menz23	*R. pendulinus*	*menzbieri*	Iran	Azerbaijan-e-Gharbi	45.25	37.4	KY694021
Rpen_menz24	*R. pendulinus*	*menzbieri*	Iran	Azerbaijan-e-Gharbi	45.25	37.4	KY694022
Rpen_menz25	*R. pendulinus*	*menzbieri*	Iran	Azerbaijan-e-Gharbi	45.25	37.4	KY694023
Rpen_menz26	*R. pendulinus*	*menzbieri*	Iran	Kordestan	46.11	35.55	KY694024
Rpen_menz27	*R. pendulinus*	*menzbieri*	Iran	Kordestan	46.11	35.55	KY694025
Rpen_menz3	*R. pendulinus*	*menzbieri*	Iran	Kordestan	46.11	35.55	KY694026
Rpen_menz4	*R. pendulinus*	*menzbieri*	Iran	Kordestan	46.11	35.55	KY694027
Rpen_menz5	*R. pendulinus*	*menzbieri*	Iran	Kordestan	46.11	35.55	KY694028
Rpen_menz6	*R. pendulinus*	*menzbieri*	Iran	Kordestan	46.11	35.55	KY694029
Rpen_menz7	*R. pendulinus*	*menzbieri*	Iran	Kordestan	46.11	35.55	KY694030
Rpen_menz8	*R. pendulinus*	*menzbieri*	Iran	Kordestan	46.11	35.55	KY694031
Rpen_menz9	*R. pendulinus*	*menzbieri*	Iran	Kordestan	46.11	35.55	KY694032
Rpen_pend_186	*R. pendulinus*	*pendulinus*	Hungary	Feherto	20.05	46.19	KY694033
Rpen_pend_277	*R. pendulinus*	*pendulinus*	Hungary	Feherto	20.05	46.19	KY694034
RppendSic_AV30408	*R. pendulinus*	*pendulinus*	Italy	Piana di Vicari	13.33	37.50	KY694035
RppendSic_AV30410	*R. pendulinus*	*pendulinus*	Italy	Piana di Vicari	13.33	37.50	KY694036
Rp_caspius_1930	*R. pendulinus*	*caspius*	Kazakhstan	South East Ural	–*	–	KY694037

genotyping errors and the presence of null alleles (null allele estimates as per the method of Brookfield 1996).

Phylogenetic analyses

The cytochrome-*b* sequences were aligned by ClustalW using MEGA 6.0 (Tamura et al. 2013). Haplotype diversity (Hd) (Nei 1987) and nucleotide diversity (π) (Lynch and Crease 1990) were calculated in the software DnaSP 5.10.01 (Librado and Rozas 2009) for four species *R. pendulinus*, *R. macronyx*, *R. coronatus*, and *R. consobrinus*. Median-joining networks were reconstructed based on the frequency of individuals carrying the different haplotypes using the PopART 1.7 (Bandelt et al. 1999).

We applied both maximum likelihood (ML) and Bayesian inference (BI) to analyze our mitochondrial cytochrome-*b* gene data in a phylogenetic context. The program ModelTest 3.07 (Posada and Crandall 1998), applying the Akaike information criterion (AIC), was used to select the best-fit nucleotide substitution model (Posada and Buckley 2004). The selected model GTR + I + G was employed in both the Bayesian inference and the maximum likelihood analyses. In the Bayesian inference analysis we ran 10 million generations (4 chains of Markov Chain Monte Carlo (MCMC) using MrBayes ver. 3.1.2 (Ronquist and Huelsenbeck 2003)). For the maximum likelihood analyses (1000-tree search replicates and non-parametric bootstrapping to estimate nodal support) we used RAxML ver. 8.0.20 (Stamatakis 2006). The burn-in and convergence diagnostics of MrBayes analysis were estimated using Tracer ver. 1.4 (Rambaut and Drummond 2007). Phylogenetic trees were visualized in FigTree 1.4.2 (Rambaut 2014).

All ten microsatellite loci were tested for Hardy Weinberg Equilibrium (HWE) and linkage disequilibrium in GENEPOP 4.4 (Rousset 2008) within *R. pendulinus* and *R. macronyx*. We used the mean number of alleles and allelic richness to quantify genetic variability in FSTAT 2.9.3 (Goudet 2001). The MCMC method (with 10 000 dememorization, 1000 batches at 10 000 iterations per batch) was used to measure the probabilities. Also, the Fisher method was used to analyze the global HWE estimates by loci and by species in GENEPOP. The model-based clustering program STRUCTURE 2.3.2 (Pritchard et al. 2000) was used to infer population structure of the closely related taxa *R. pendulinus* and *R. macronyx*. We applied a burn-in of 100 000, run length of 1 000 000, and a model allowing for admixture model and correlated allele frequencies mode with sampling location information. This was run 10 times for each K (1–5) without any prior information on the population of origin of each individual. We excluded loci that were not under the HWE and contained null for STRUCTURE analyses. We used Structure Harvester ver. 0.6.94 (Earl and von Holdt 2012) to identify the most likely number of genetic clusters on the basis of the ad-hoc statistics described in Evanno et al. (2005).

Genetic distances were calculated as outlined in the GENALEX 6.5 (Peakall and Smouse 2006) guide for codominant data. To visualize the genetic structure between the individuals included in the microsatellite genotyping we also conducted a principal coordinate analysis (PCoA) based on inter-individual genetic distance and applied AMOVAs on pairwise Φ_{PT} (cytochrome-*b*) and F_{ST} values (microsatellites) in GENALEX.

Data deposition

Data available from the Dryad Digital Repository: <http://dx.doi.org/10.5061/dryad.r5728> (Barani-Beiranvand et al. 2017).

Results

Mitochondrial genes

The cytochrome-*b* alignment consisted of 843 bp. Of the 45 polymorphic sites, 37 sites were phylogenetically informative and eight were singletons. We observed 16 common haplotypes among the four morphologically differentiated species of the genus *Remiz* (*R. pendulinus*, *R. macronyx*, *R. coronatus*, and *R. consobrinus*). Median-joining haplotype network detected three lineages (Fig. 2). The *R. pendulinus* and *R. macronyx* haplotypes occupied a central position in the network and were clearly differentiated from the *R. coronatus*, and *R. consobrinus* clades (each with 12 and 24 mutational steps, respectively) (Fig. 2, Supplementary material Appendix 2). Overall, the species' haplotype (Hd) and nucleotide (π) diversities were 0.603 ± 0.07 and 0.009 ± 0.002, respectively (Table 1). The Bayesian gene trees identified three well-supported clades (I–III) within the genus *Remiz* (Fig. 3). The support for the internal nodes in clade I, including *R. pendulinus* and *R. macronyx,* was low (posterior probability < 0.95). The main topology of the ML tree (not shown) was identical to the BI tree, and recovered the same three major clades. The minimum genetic distance between pairs of individuals referred to *R. macronyx* and *R. pendulinus* was 0.001 while the maximum divergence between *R. consobrinus* and the other three species was 0.041 (Table 2). The genetic distance between *R. coronatus* with *R. macronyx* and *R. pendulinus* was about the same (0.017 and 0.018 respectively; Table 3). The Φ_{PT}-value based on 999 permutations for cytochrome-*b* was 0.451 ($p \leq 0.001$) between four species (Table 3).

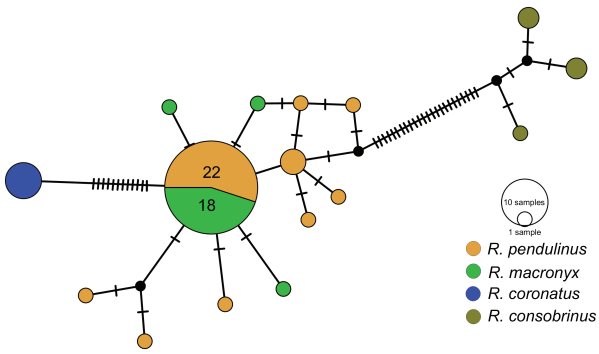

Figure 2. Cytochrome-*b* median-joining network. Median-joining network among the genus *Remiz* haplotypes. Each circle represents a different haplotype or group of haplotypes with size proportional to their relative frequency. Differences between haplotypes are proportional to branch length and mutational steps. The numbers in main shared haplotype network indicate individual frequency.

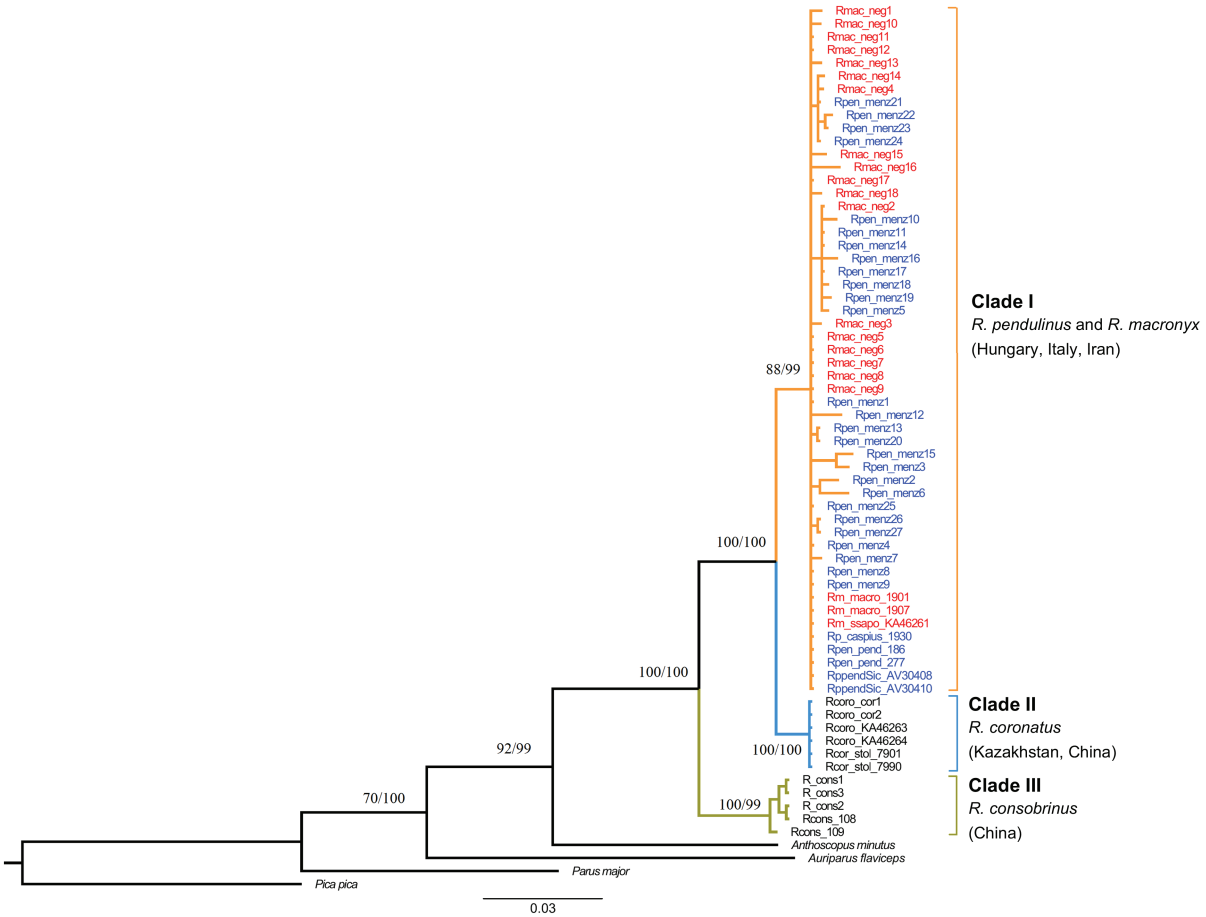

Figure 3. Phylogram of the cytochrome-*b* sequences of the genus *Remiz* using Bayesian inference. All major nodes are highly supported, while in the clade I internal nodes were unable to separate *R. macronyx* from *R. pendulinus*. Bootstrap values of the ML and posterior probability of BI analyses are represented on the branches, respectively.

Microsatellite markers

In the ten microsatellite loci, the number of alleles ranged from three to seven and the observed and expected heterozygosity ranged from 0.190 to 0.856 and 0.141 to 0.711, respectively (Supplementary material Appendix 1). Microchecker indicated no significant genotyping errors while loci Rem-09 (0.1839) and TG-053 (0.1212) in *R. pendulinus* and loci Rem-09 (0.1946) and TG-009 (0.0387) in *R. macronyx* (after Bonferonni correction at the 5% nominal level) showed signs of a null allele. The results of the HWE analyses in GENEPOP were as follows: in *R. pendulinus* (Rem-09: $F = 0.559$, $p = 0.0002$; TG-053: $F = 0.292$, $p = 0.0109$) and in *R. macronyx* (Rem-09: $F = 0.5467$, $p = 0.0001$; TG-053: $F = -0.1879$, $p = 0.0185$). In the linkage disequilibrium test, in *R. pendulinus* two pairs and in *R. macronyx* seven pairs of loci were significantly linked ($p \leq 0.05$). Therefore, the populations were not in HWE and we removed Rem-09, TG-053, and TG-009 in the STRUCTURE analyses. *Remiz macronyx* had a lower allelic richness (3.78) than *R. macronyx* (4.38), with mean number of alleles 3.8 and 5.2, respectively. Microsatellite markers yielded a capacity to discriminate among the two taxa analyzed (Fisher's test, $Chi2 = 68.225$, $df = 36$, $p = 0.0009$).

When analyzing the 44 adult individuals in STRUCTURE (after excluding loci that were not under the HWE and contain null alleles), we got a mean Ln probability of –632.2, supporting $K = 2$ (Fig. 4A), while Evanno's method (6.462) supported $K = 3$ (Fig. 4B). The two genetic clusters suggested by the standard method corresponds *R. pendulinus*

Table 2. The genus *Remiz*, sample size, genetic diversity based on cytochrome-*b* sequences in Palearctic region. n, the number of individuals sequenced; n_h, haplotype number; n_p, number of polymorphic sites; Hd, haplotype diversity; π, nucleotide diversity; and SD, standard deviation.

Species	n	nh	np	Hd (± SD)	π (± SD)	Region
R. pendulinus	32	16	19	0.784 (0.077)	0.002 (0.006)	Hungary, Italy, Iran
R. macronyx	21	5	4	0.352 (0.131)	0	Kazakhstan, Iran
R. coronatus	6	1	0	0	0	Kazakhstan, China
R. consobrinus	5	3	4	0.800 (0.164)	0.002 (0.000)	China
			Total	0.603 (0.071)	0.009 (0.002)	

Table 3. Genetic structure over sequence pairs for cytochrome-*b* between four species of the genus *Remiz*. Average genetic distance over all sequence pairs between species are shown in lower left. Φ_{PT} values are shown above diagonal (*: $p \leq 0.004$, **: $p \leq 0.001$ based on 999 permutations).

Species	*R. consobrinus*	*R. coronatus*	*R. macronyx*	*R. pendulinus*
R. consobrinus	–	0.935**	0.625**	0.739**
R. coronatus	0.041	–	0.447**	0.586**
R. macronyx	0.041	0.017	–	**0.054***
R. pendulinus	0.041	0.018	**0.001**	–

and *R. macronyx*, respectively (Fig. 4C). The three cluster result suggested using Evanno's method did not correspond to any pre-defined groups but instead showed an admixed structure (figure not shown). As a two-cluster division was also found in the PCoA analysis of the microsatellite data, where the individuals of *R. pendulinus* and *R. macronyx* were slightly differentiated (Fig. 5), we rely on the result (K = 2) revealed by standard mean method.

The mean F_{ST}-value between *R. pendulinus* and *R. macronyx* for all microsatellite markers based on 1000 permutations was 0.072 ($p \leq 0.01$) indicating gene flow and limited genetic differentiation between these two taxa (Table 4). The variation among populations in these taxa was 7.27% (Table 4). The observed and expected heterozygosity and their significance levels are shown in Supplementary material Appendix 3.

Discussion

Here, we provide a comprehensive molecular study of the genus *Remiz* using a combination of mitochondrial and microsatellite markers to study the phylogenetic relationships and species boundaries within this genus. The mitochondrial data strongly support the proposition that *R. coronatus*, *R. consobrinus*, and *R. pendulinus*/*macronyx* form three independent evolutionary lineages, while microsatellite genotyping supported the notion that *R. pendulinus* and *R. macronyx* are also differentiated, albeit marginally. The three main linages (*R. coronatus*, *R. consobrinus*, and *R. pendulinus*/*macronyx*) can not only be genetically differentiated, but also based on morphology, behaviour and the type of habitat they inhabit (Harrap and Quinn 1996, Madge 2008, Bot and van Dijk 2009, Bot et al. 2011). Ivanov (1940) pointed out

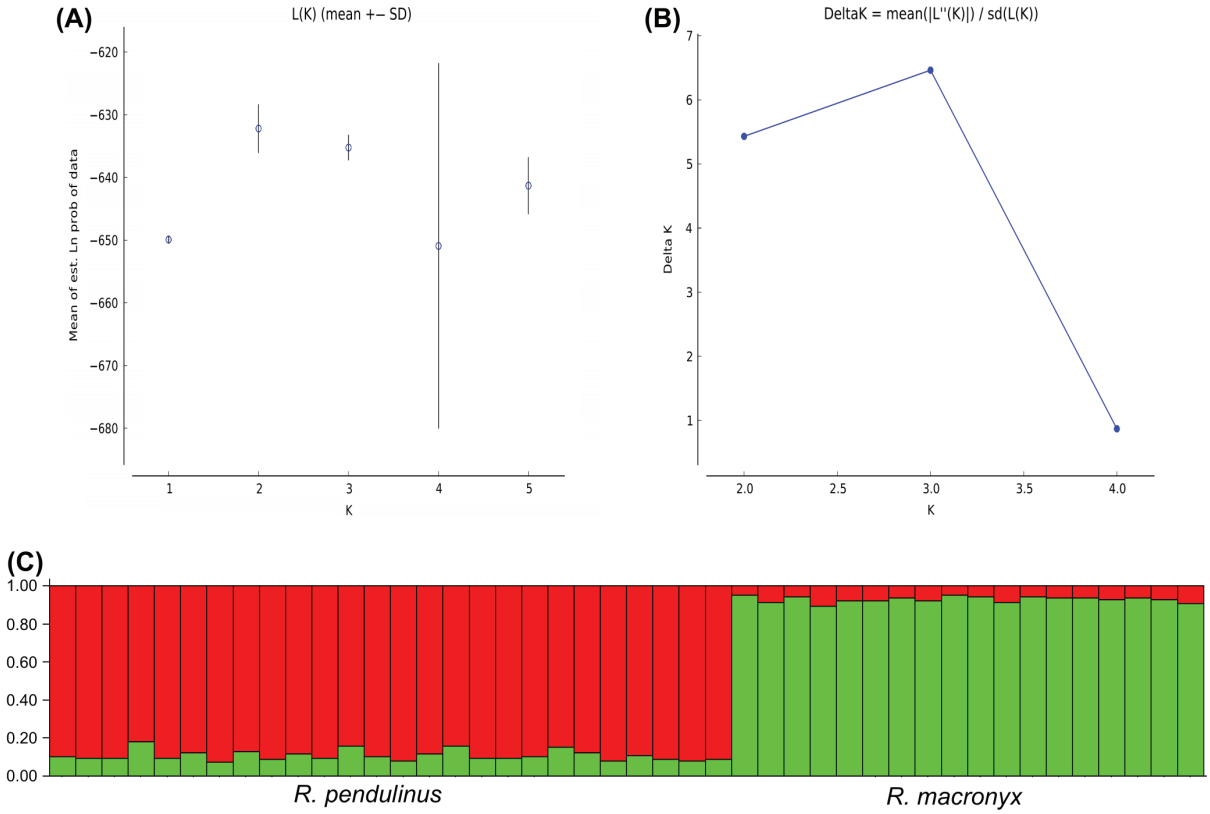

Figure 4. Visualisations of the STRUCTURE results for *R. pendulinus* (n = 26) and *R. macronyx* (n = 18) in two allopatric area in Iran, based on seven microsatellite loci (after excluding loci that were not under the HWE and contain null alleles), showing (A) the mean likelihood of the observed data given each number of clusters (K) and the corresponding variance, (B) the rate of change in the log probabilities (Delta K) based on the Evanno et al. (2005), and (C) the assignment of the individual to the two clusters at K = 2 including information of the sampling location as a prior in admixture model. Each vertical line represents one individual and each colour represents a single cluster. The vertical height of each colour represents the probability of being with a single cluster. Note that there is clear difference in the assignment probabilities between two taxa.

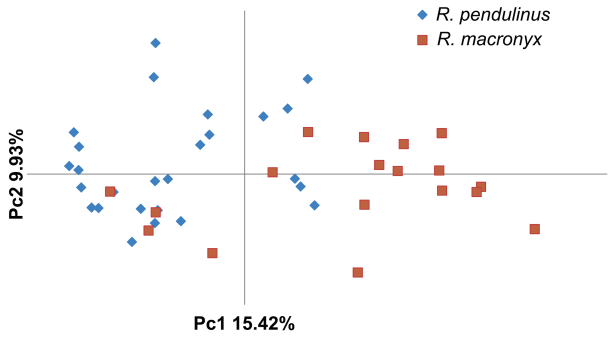

Figure 5. Principal coordinate analysis (PCoA) plot for individuals from two allopatric taxa *R. pendulinus* and *R. macronyx* analysed with ten microsatellite loci.

that breeding ranges of *R. coronatus* meet with *R. pendulinus* and *R. macronyx* in western Tajikistan. He encountered *R. coronatus* in willow (*Salix*) and birch (*Betula*), whilst the two other species only inhabited *Phragmites* reedbeds, with no evidence of interbreeding (Madge 2008).

Our genetic results are concordant with Sibley and Monroe (1990) that lumped *R. pendulinus* with *R. macronyx*, but are inconsistent with Cramp and Perrins (1993) and Dickinson and Christidis (2014) that considered *R. coronatus* and *R. consobrinus* as conspecific. Eck and Martens (2006) believed the *macronyx* subspecies is part of the species *pendulinus* and explained that relationships between *coronatus* and *consobrinus* are not clearly resolved. They preferred to treat *coronatus* and *consobrinus* under the species *Remiz consobrinus* until more data would become available. Bot and van Dijk (2009) showed significant differences between *R. coronatus* and *R. macronyx* in biometry, vocalization and plumage traits. Their field observations are in agreement with our results based on the molecular genetics of the two species.

Although genetic differentiation between *R. pendulinus* and *R. macronyx* appears to be low, these taxa are generally very different in morphology (Madge 2008, Bot et al. 2011). In *R. pendulinus*, the male has a black mask extending backwards, a light grey nape, chestnut-coloured mantle and upperwing-coverts, and often some chestnut-coloured spots on the breast. In contrast, in a typical *R. macronyx*, the male's entire head, throat and upper breast are sooty black, mantle and upper scapulars chestnut coloured, upperwing feathers reddish-brown or blackish, and the sides of breast chestnut (Madge 2008). This suggests that although this complex may have started to diverge only recently, there has been a strong selection on phenotypes. However, our data cannot discriminate whether the lack of prominent molecular differentiation is due to *R. pendulinus* and *R. macronyx* constituting very young taxa, to secondary contact and hybridization, or to a combination of both. However, the observations of individuals with phenotypes of intermediate appearance at our study site near Topar, Kazakhstan (Bot and van Dijk 2009, Bot et al. 2011) suggest that hybridization could at least partially explain this pattern. Additionally, gene expression research suggests that sequence data may contain limited information on the origin of important phenotypic differences between sister taxa (Tautz 2000, Laland et al. 2015). Genomic studies of, for example, crows *Corvus corone* (Poelstra et al. 2014) suggest that very narrow genomic regions may constitute barriers to gene flow and could result in phenotypic differences that are important for mate-choice. Thus, localized genomic selection can cause marked heterogeneity in introgression landscapes while maintaining phenotypic divergence. Thus, we cannot exclude the possibility that the investigated genetic markers may have been too few, failing to detect population genetic divergence, and that the phenotypic diversity may, at least in part, be due to differences in gene expression.

Our results show that the *R. pendulinus* and *R. macronyx* complex are among the small, but growing list of species complexes for which low levels of genetic differentiation are accompanied by the presence of strong phenotypic divergence. Examples include crows *Corvus corone* (Poelstra et al. 2014), Darwin's finches *Geospiza* spp. and *Camarhynchus* spp. (Lamichhaney et al. 2015), redpolls *Acanthis* spp. (Mason and Taylor 2015), tyrant-flycatchers *Zimmerius* spp. (Rheindt et al. 2008), and Kentish plovers *Charadrius* (Rheindt et al. 2011). These studies thus highlight the need for further, comparative genomic studies aiming to understand how phenotypic divergence contributes to speciation (Price 2008).

In conclusion, using DNA sequences of mitochondrial and microsatellite markers we show that at least three species should be recognized within the genus *Remiz*: *R. pendulinus*, *R. coronatus*, and *R. consobrinus*. Additionally, despite extensive phenotypic differences, microsatellite genotyping suggests that *R. macronyx* is only marginally differentiated from *R. pendulinus*. This result suggests that these two taxa may be at an early stage of speciation. However, the alternative explanation of secondary contact and hybridization resulting in extensive gene flow cannot be excluded. Taken together, our results are congruent with known variation in morphology, behaviour and ecology of penduline tits and suggest that Remizidae represents a diverse and rapidly radiating clade.

Table 4. Overall Φ_{PT} value for cytochrome-*b* among and between four species of the genus *Remiz* and overall F_{ST} value for microsatellite markers in two taxa of *R. pendulinus* and *R. macronyx* ($p \leq 0.001$). SM: sum of squares, MS: mean of squares.

	Mitochondrial analysis					Microsatellite analysis				
Source	df	SS	MS	Est.Var.	Var. (%)	df	SS	MS	Est.Var.	Var. (%)
Among Taxa	3	259.541	86.514	5.924	0.45	1	10.524	10.524	0.19	0.07
Within Taxa	60	432.881	7.215	7.215	0.55	86	209.408	2.435	2.435	0.93
Total	63	692.422		13.139	1	87	219.932		2.625	1
	PhiPT = 0.451	$p \leq 0.001$				$F_{ST} = 0.072$	$p \leq 0.001$			

Acknowledgements – We thank Alexander Ball for providing cytochrome-*b* sequences of *Remiz coronatus*. We also thank the people who assisted with the fieldwork: Sander Bot, Dušan Brinkhuizen, Natalino Cuti, Bruno Massa, Ákos Pogány, Sergey Sklyarenko and Vera Voronova. The Swedish Museum of Natural History (NRM) is acknowledged for providing laboratory facilities and technical support.

Funding – The study was financially supported by project no. 3/24104 in Ferdowsi Univ. of Mashhad (FUM) to HB-B, by Ministry of Science, Research and Technology of Iran (grant number: 3/23089) to MA, and the Swedish Research Council (grant number 621-2013-5161 to PE and grant number 621-2014-5113 to MI). This research leading to these results has also received funding from the European Community's Sixth Framework Programme (GEBACO; FP6/2002-2006) under contract number 28696.

Permissions – The Dept of Environment (DOE) is acknowledged for providing the permits and logistical support for fieldwork in Iran.

References

Bandelt, H. J., Forster, P. and Röhl, A. 1999. Median-joining networks for inferring intraspecific phylogenies. – Mol. Biol. Evol. 16: 37–48.

Barani-Beiranvand, H., Aliabadian, A., Irestedt, M., Qu, Y., Darvish, J., Szekely, J. D., van Dijk, R. E. and Ericson, P. G. P. 2017. Data from: Phylogeny of penduline tits inferred from mitochondrial and microsatellite genotyping. – Dryad Digital Repository, <http://dx.doi.org/10.5061/dryad.r5728>.

Bot, S. and van Dijk, R. E. 2009. Black-headed penduline tits *Remiz macronyx* in Kazakhstan. – Sandgrouse 31: 171–176.

Bot, S., Brinkhuizen, D., Pogány, Á., Székely, T. and van Dijk, R. E. 2011. Penduline tits in Eurasia: distribution, identification and systematics. – Dutch Birding 33: 177–187.

Brookfield, J. 1996. A simple new method for estimating null allele frequency from heterozygote deficiency. – Mol. Ecol. 5: 453–455.

Cramp, S. and Perrins, C. 1993. The birds of the Western Palearctic, vol. 8–9. – Oxford Univ. Press.

Dawson, D. A., Horsburgh, G. J., Küpper, C., Stewart, I. R., Ball, A. D., Durrant, K. L., Hansson, B., Bacon, I., Bird, S. and Klein, A. 2010. New methods to identify conserved microsatellite loci and develop primer sets of high cross-species utility – as demonstrated for birds. – Mol. Ecol. Resour. 10: 475–494.

Dawson, D. A., Ball, A. D., Spurgin, L. G., Martín-Gálvez, D., Stewart, I. R., Horsburgh, G. J., Potter, J., Molina-Morales, M., Bicknell, A. W. and Preston, S. A. 2013. High-utility conserved avian microsatellite markers enable parentage and population studies across a wide range of species. – BMC Genomics 14: 176.

Dickinson, E. 2003. The Howard and Moore complete checklist of the birds of the world. – Christopher Helm.

Dickinson, E. and Christidis, L. 2014. The Howard and Moore complete checklist of the birds of the world, vol. 2. Passerines, 4th ed. – Aves Press.

Earl, D. A. and von Holdt, B. M. 2012. Structure Harvester: a website and program for visualizing STRUCTURE output and implementing the Evanno method. – Conserv. Genet. Resour. 4: 359–361

Eck, S. and Martens, J. 2006. Systematic notes on Asian birds. 49. A preliminary review of the Aegithalidae, Remizidae and Paridae. – Zool. Med. 80: 1–63.

Evanno, G., Regnaut, S. and Goudet, J. 2005. Detecting the number of clusters of individuals using the software STRUCTURE: a simulation study. – Mol. Ecol. 14: 2611–2620.

Goudet J. 2001. FSTAT, a program to estimate and test gene diversities and fixation indices. – Version 2.9.3.

Harrap, S. and Quinn, D. 1996. Tits, nuthatches and treecreepers. – A. and C. Black.

Isenmann, P. 1987. Zur Ausbreitung der Beutelmeise (*Remiz pendulinus*) in Westeuropa: die Lage an der südwestlichen Verbreitungsgrenze. – J. Ornithol. 128: 110–111.

Ivanov, A. I. 1940. Ptitsy Tadjikistana (Birds of Tadjikistan). – AN SSSR. Tadzh. baza. Trudy (Proc. of Tadjik base) Zool. Parasithol. 10: 292–295.

Laland, K. N., Uller, T., Feldman, M. W., Sterelny, K., Müller, G. B., Moczek, A., Jablonka, E. and Odling-Smee, J. 2015. The extended evolutionary synthesis: its structure, assumptions and predictions. – Proc. R. Soc. B 282: 1019.

Lamichhaney, S., Berglund, J., Almén, M. S., Maqbool, K., Grabherr, M., Martinez-Barrio, A., Promerová, M., Rubin, C. J., Wang, C., Zamani, N. and Grant, B. R. 2015. Evolution of Darwin's finches and their beaks revealed by genome sequencing. – Nature 518: 371–375.

Librado, P. and Rozas, J. 2009. DnaSP v5: a software for comprehensive analysis of DNA polymorphism data. – Bioinformatics 25: 1451–1452.

Lynch, M. and Crease, T. 1990. The analysis of population survey data on DNA sequence variation. – Mol. Biol. Evol. 7: 377–394.

Madge, S. 2008. Family Remizidae (penduline-tits). – In: del Hoyo, J., Elliott, A. and Christie, D. (eds), Handbook of birds of the world, vol. 13, penduline-tits to shrikes. Lynx Edicions, pp. 52–75.

Mason, N. A. and Taylor, S. A. 2015. Differentially expressed genes match bill morphology and plumage despite largely undifferentiated genomes in a Holarctic songbird. – Mol. Ecol. 24: 3009–3025.

Mészáros, L. A., Frauenfelder, N., van der Velde, M., Komdeur, J. and Szabad, J. 2008. Polymorphic microsatellite DNA markers in the penduline tit, *Remiz pendulinus*. – Mol. Ecol. Resour. 8: 692–694.

Nei, M. 1987. Molecular evolutionary genetics. – Columbia Univ. Press.

Newton, I. 2010. The migration ecology of birds. – Academic press.

Ottvall, R., Bensch, S., Walinder, G. and Lifjeld, J. T. 2002. No evidence of genetic differentiation between lesser redpolls *Carduelis flammea* cabaret and common redpolls *Carduelis f. flammea*. – Avian Sci. 2: 237–244.

Peakall, R. and Smouse, P. E. 2006. GENALEX 6: genetic analysis in Excel. Population genetic software for teaching and research. – Mol. Ecol. Notes 6: 288–295.

Persson, O. and Öhrström, P. 1989. A new avian mating system: ambisexual polygamy in the penduline tit *Remiz pendulinus*. – Ornis Scand. 20: 105–111.

Poelstra, J. W., Vijay, N., Bossu, C. M., Lantz, H., Ryll, B., Müller, I., Baglione, V., Unneberg, P., Wikelski, M. and Grabherr, M. G. 2014. The genomic landscape underlying phenotypic integrity in the face of gene flow in crows. – Science 344: 1410–1414.

Portenko, L. A. 1955. New subspecies of passerine birds (Aves, Passeriformes). – Tr. Zool. Inst. Akad. Nauk. USSR 18: 493–507

Posada, D. and Crandall, K. A. 1998. Modeltest: testing the model of DNA substitution. – Bioinformatics 14: 817–818.

Posada, D. and Buckley, T. R. 2004. Model selection and model averaging in phylogenetics: advantages of Akaike information criterion and Bayesian approaches over likelihood ratio tests. – Syst. Biol. 53: 793–808.

Price, T. 2008. Speciation in birds. – Roberts, Greenwood Village, CO.

Pritchard, J. K., Stephens, M. and Donnelly, P. 2000. Inference of population structure using multilocus genotype data. – Genetics 155: 945–959.
Rambaut, A. 2014. FigTree 1.4. 2. – Univ. of Edinburgh, <http://tree.bio.ed.ac.uk/software/figtree>.
Rambaut, A. and Drummond, A. J. 2007. Tracer v1.4. – <http://beast.bio.ed.ac.uk/Tracer>.
Rheindt, F. E., Norman, J. A. and Christidis, L. 2008. DNA evidence shows vocalizations to be a better indicator of taxonomic limits than plumage patterns in *Zimmerius* tyrant-flycatchers. – Mol. Phylogenet. Evol. 48: 150–156.
Rheindt, F. E., Székely, T., Edwards, S. V., Lee, P. L., Burke, T., Kennerley, P. R., Bakewell, D. N., Alrashidi, M., Kosztolányi, A. and Weston, M. A. 2011. Conflict between genetic and phenotypic differentiation: the evolutionary history of a 'lost and rediscovered' shorebird. – PLoS One 6: e26995.
Ronquist, F. and Huelsenbeck, J. P. 2003. MrBayes 3: Bayesian phylogenetic inference under mixed models. – Bioinformatics 19: 1572–1574.
Rousset, F. 2008. GENEPOP'007: a complete re-implementation of the GENEPOP software for Windows and Linux. – Mol. Ecol. Resour. 8: 103–106.
Sibley, C. G. and Monroe, B. L. 1990. Distribution and taxonomy of birds of the world. – Yale Univ. Press.
Snow, D. 1967. The families Aegithalidae, Remizidae and Paridae. Check-list of birds of the World. A continuation of the work of James L. Peters. – Harvard Univ. Press.
Stamatakis A. 2006. RAxML-VI-HPC: maximum likelihood-based phylogenetic analyses with thousands of taxa and mixed models. – Bioinformatics 22: 2688–2690.
Szentirmai, I., Székely, T. and Komdeur, J. 2007. Sexual conflict over care: antagonistic effects of clutch desertion on reproductive success of male and female penduline tits. – J. Evol. Biol. 20: 1739–1744.
Tamura, K., Stecher, G., Peterson, D., Filipski, A., Dudley, J., Nei, M. and Kumar, S. 2013. MEGA6: molecular evolutionary genetics analysis version 6.0. – Mol. Biol. Evol. 30: 2725–2729.
Tautz, D. 2000. Evolution of transcriptional regulation. – Curr. Opin. Genet. Dev. 10: 575–579.
van Dijk, R. E., Mészáros, L. A., van der Velde, M., Székely, T., Pogány, Á., Szabad, J. and Komdeur, J. 2010a. Nest desertion is not predicted by cuckoldry in the Eurasian penduline tit. – Behav. Ecol. Sociobiol. 64: 1425–1435.
van Dijk, R. E., Pogány, Á., Komdeur, J., Lloyd, P. and Székely, T. 2010b. Sexual conflict predicts morphology and behavior in two species of penduline tits. – BMC Evol. Biol. 10: 107.
van Dijk, R. E., Komdeur, J. and Székely, T. 2012. Nest attendance does not predict offspring desertion by Eurasian penduline tit parents. – Ethology 118: 703–710.
van Oosterhout, C., Hutchinson, W. F., Wills, D. P. and Shipley, P. 2004. MICRO-CHECKER: software for identifying and correcting genotyping errors in microsatellite data. – Mol. Ecol. Notes 4: 535–538.

Supplementary material (Appendix JAV-01163 at <www.avianbiology.org/appendix/jav-01163>). Appendix 1–3.